# Specific heat of thin-film $A15$ superconductors: An anomalous inhomogeneity discovered

F. Hellman* and T. H. Geballe†
*Department of Applied Physics, Stanford University, Stanford, California 94305*
(Received 9 January 1987)

Thin films of metallurgically stable $A15$ superconductors, primarily Nb-Sn, V-Ga, and V-Si, have been prepared by electron-beam coevaporation onto heated sapphire substrates. The specific heat of these films at low temperature reveals that the width of the transition from the normal to the superconducting state varies from a low of 0.3 K for stoichiometric $Nb_3Sn$ to a high of 6 K for $A15$ Nb-Sn prepared off-stoichiometry. The systematics of this transition width were probed by varying the deposition parameters. A strong dependence is found on deposition temperature, composition, and microstructure. The source appears to be a compositional inhomogeneity which develops at the film surface during growth. A model is proposed for a new type of surface segregation applicable in a growing film where the surface mobility is orders of magnitude greater than the bulk mobility.

## INTRODUCTION

Materials which form with the $A15$ crystal structure are well-known high-$T_c$ superconductors. Their high critical temperature $T_c$, together with large superconducting gaps, large critical fields, and generally high critical currents, make these materials of technological interest. These compounds are generally written $A_{1-x}B_x$, where, typically, $A$ is Nb or V and $B$ is Sn, Ga, Si, Al, or Ge. For a stoichiometric compound, $x=0.25$; if the compound is ordered, the $B$ atoms occupy bcc sites and the $A$ atoms occupy sites in nonintersecting chains along the cube faces. Most of the compounds are metallurgically stable over a range of $x$, which may or may not include $x=0.25$. Reference 1 contains a review of the phase diagrams of the $A15$ compounds. Thin films, grown by vapor deposition, are necessary for certain applications. In addition, thin films of $A15$ superconductors have been used for many of the measurements made in pursuit of a fundamental understanding of superconductivity in strong electron-phonon–coupled materials in general and of the cause of the high transition temperatures in the $A15$ materials in particular.

The specific heat of various $A15$ superconductors has been measured and analyzed for bulk samples.[2–9] In this study, we report on the first measurements of specific heat done directly on as-deposited thin-film samples. The purpose of measuring the specific heat of the thin films was originally twofold. First, some of the highest-$T_c$ $A15$ materials, such as $Nb_3Ge$, are metastable and are most readily prepared by thin-film techniques such as quenching from the vapor. Some others of the $A15$ class, such as Nb-Sn, are metallurgically stable, but have phase diagrams which make it difficult to prepare homogeneous bulk samples at all compositions. Vapor-phase deposition under ideal circumstances gives an extremely homogeneous mixture. Furthermore, specific heat is a reliable probe of the homogeneity of the transition temperature of a material, which in the $A15$ compounds translates directly into a probe of the homogeneity, for length scales greater than the superconducting coherence length, of such material properties as composition, impurities, disorder, and strain. The second reason for measuring the specific heat on thin films is that many of the fundamental measurements on the $A15$ compounds are performed on thin-film samples. It is therefore preferable to determine the microscopic parameters available from analysis of specific-heat data on the very same samples. In light of the results to be presented in this paper, this second purpose was postponed.

The films are grown by electron-beam coevaporation onto heated substrates. Films thus prepared have been much studied from both a microstructural and a superconducting point of view. It was believed that optimized deposition procedures had been found, at least for the $A15$ compound $Nb_3Sn$. However, upon measuring the specific heat of a variety of $A15$ compounds, an anomalous inhomogeneity in the superconducting transition temperature was observed. This inhomogeneity is greatest in the Nb-Sn system, the system believed to be the most stable and best understood of the high-$T_c$ $A15$ materials. The systematics of the inhomogeneity were probed by varying the deposition parameters, such as film composition, substrate temperature, deposition rate, and background gases, and by annealing. Only the $A15$ compounds believed to be metallurgically stable, primarily Nb-Sn, V-Si, and V-Ga, are included in this study. The observed results strongly suggest a compositional inhomogeneity which develops at the surface during the growth of the film despite a homogeneous deposition. A model for a new manifestation of surface segregation, applicable in a growing film where the surface mobility is orders of magnitude greater than the bulk mobility, is developed to explain the results.

## SAMPLE PREPARATION AND CHARACTERIZATION

The films, which are typically 2–2.5 $\mu$m thick, are grown on $(1\bar{1}02)$ $(\frac{1}{4}\times\frac{1}{4})$-in.$^2$ nominally epitaxially pol-

 

ished sapphire substrates in an electron-beam evaporator designed by Hammond.[10,11] Two $A$-element sources with a $B$-element source between them (arranged linearly) are used in order to essentially eliminate any geometry-related composition spread across the samples and to greatly reduce any shadowing. This arrangement results in a single composition per evaporation. The rate from each source is individually monitored by chopped ionization-gauge rate monitors. The signal from each rate monitor is fed into a lock-in amplifier. The deviation from the desired rate is then fed back to the electron-gun controller for that source. The resulting rates are believed constant within 1%. Background pressure during the evaporation varies from $2\times10^{-8}$ to $2\times10^{-7}$ Torr and is primarily methane. Substrates are clamped to a polished Nb block by means of 0.015-in. Mo clips. This block may be heated to any temperature up to 1100 °C or cooled to liquid-nitrogen temperatures. For the Nb-Sn system, previous work had found that temperatures between 750 and 850 °C produce well-ordered material, with no Sn loss during evaporation.[12–16] Rates of 10–30 Å/sec yield optimal rate control. In addition, the tradeoff between slow depositions to allow ordering and the resulting increase in incorporated background-gas impurities is a factor in the choice of rate. Similar deposition parameters were chosen for the other $A15$ materials. For more details of sample preparation, see Ref. 15 or 16.

Films thus prepared have been extensively characterized. Among the measurements made are inductive and resistive $T_c$,[12,15–18] transmission-electron microscopy (TEM),[14,18–20] x-ray diffraction,[12,15,17] sputtering Auger profile,[15] resistivity,[13,14,16] superconductive tunneling,[12,15,17,21] superconductive critical currents and fields,[13,14,18,22] and rf surface losses.[23]

The specific-heat experiment was designed by Early for the purpose of measuring submilligram samples.[24] It is especially suitable for the measurement of thin films which are deposited directly onto the back side of a 0.005-in.-thick silicon-on-sapphire substrate. This substrate should be identical to the sapphire substrates used for the other measurements in all aspects except the reduced thickness. The front of the substrate contains the doped photolithographically patterned Si thermometers and heater used to make the specific-heat measurement. The measurement is made by the relaxation method. The estimated error is 5% in the sample heat capacity plus an additional 5% in the specific heat due to uncertainty in the sample weight. See Refs. 16, 24, and 25 for more detail.

## RESULTS

Figure 1 shows the specific heat of six $A15$ Nb-Sn samples with compositions spanning the accepted equilibrium phase field. The lines are drawn to guide the eye and are not theoretical fits. For clarity, several samples with intermediate compositions are not included in this figure. These samples were prepared under "standard" deposition conditions: substrate temperature $T_s$ of 800±30 °C and deposition rate of 10–20 Å/sec. We will primarily be concerned with the width of the superconducting transition temperature; for a discussion of the microscopic information available from the specific heat, such as the electron and phonon densities of states, see Ref. 16.

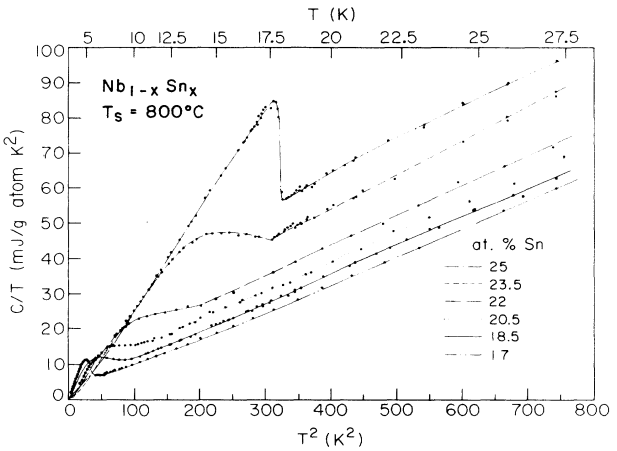


FIG. 1. Specific heat for six samples of $A15$ Nb-Sn spanning the phase field. The samples were grown under standard deposition conditions: $T_s=770$–830 °C, deposition rate of 10–20 Å/sec, $P<2\times10^{-7}$ Torr. Lines are drawn through data to guide the eye.

The specific heat of the stoichiometric film exhibits classic strong-coupled behavior. The values below 20 K are within 2% of bulk literature values; those above 20 K are within 4%.[5,26] The transition onset is 18.0 K and the transition width is 0.3 K. This transition temperature and width are quite comparable with the data presented in the literature on bulk stoichiometric samples.[2,5,6,9] By contrast, the transition temperatures measured by specific heat of the Sn-poor films are quite broad. The breadth of the transition is greatest for the 22-at. % Sn sample, 5–6 K, and decreases towards each phase boundary. Surprisingly, there is only one measurement of off-stoichiometric Nb-Sn bulk material reported in the literature Vieland and Wickland measured a 20-at. % Sn sample with a sharp (0.5 K) transition and a $T_c$ onset of 8 K.[2] Figure 2 shows the specific heat of a second 22-at. % Sn sample; the dashed line shows the data for the 22-at. % Sn sample shown in Fig. 1. The two 22-at. % Sn samples were prepared two years apart, one at 12 Å/sec and $P=1\times10^{-7}$ Torr and one at 20 Å/sec and $3\times10^{-7}$ Torr, yet the results are virtually indistinguishable.

The transition width is defined as follows. In the normal state, $C_p$ can generally be written as $\gamma T+\beta T^3+\delta T^5$ for $T<\Theta_D/10$, where $\gamma T$ is the electronic specific heat and $\beta T^3+\delta T^5$ is due to the lattice. Since $T_c$ in the Nb-Sn system is never greater than 18 K and $\Theta_D\gtrsim330$ K,[2,4–9,16] the specific-heat data were fitted to a polynomial between 18 and 35 K. The onset of $T_c$ is then taken as the temperature at which the $C_p/T$ data deviate from this fit. The specific heat at low temperatures, where all material is superconducting, must be written as a sum of the lattice specific heat, which still may be written $\beta T^3+\delta T^5$, and the electronic specific heat in the superconducting state, $C_{es}$. Even in a homogeneous material, $C_{es}$ is not a simple function of temperature, due to the fact that the

size of the superconducting gap itself is a function of temperature. Parks[27] and Daams and Carbotte[28] contain good discussions of the specific heat in the superconducting state. From a figure in the paper by Daams and Carbotte, it may be seen that between approximately $0.6T_c$ and $T_c$, $C_{es}/T$ versus $T^2$ is approximately linear for both strong- and weak-coupled superconductors, due to the details of the various contributions to the temperature dependence. In an inhomogeneous material, $C_{es}$ must be written as a sum of contributions from regions which have different $T_c$, $\gamma$, and electron-phonon–coupling constant $\lambda_{e\text{-ph}}$. The proximity effect will further complicate this sum. For simplicity, the lower end of the transition was therefore taken to be the temperature at which $C_p/T$ was clearly deviating negatively from a straight line in $T^2$. The breadth of $T_c$ and the construction used to determine it are shown in Fig. 2 for a representative sample.

This obviously imprecise definition is necessitated by the complexity of the problem. Even in the homogeneous stoichiometric material, a straightforward fit to the data above $T_c$ causes the calculated entropy in the normal state to be far larger at $T_c$ than the entropy in the superconducting state, violating thermodynamic requirements. This fact introduces an extremely large uncertainty into the lattice specific heat, the electronic specific-heat coefficient $\gamma$, and the electron-phonon–coupling corrections, as described in all references to the specific heat of A15 $Nb_3Sn$.[2,4–9,16] This uncertainty makes unambiguous determination of the lattice specific heat below $T_c$ virtually impossible. In low-$T_c$ A15 Nb-Sn, the straightforward fit yields too *small* an entropy at $T_c$.[16] Near 22 at. % Sn, the straightforward fit yields the correct entropy;[16] however, this fact should *not* be taken to mean that the lattice specific heat of a 22–at. % Sn sample is now understood. Nevertheless, as a best effort, the data for the two 22–at. % Sn samples shown in Fig. 2, which have the broadest transitions measured, were fitted in more detail

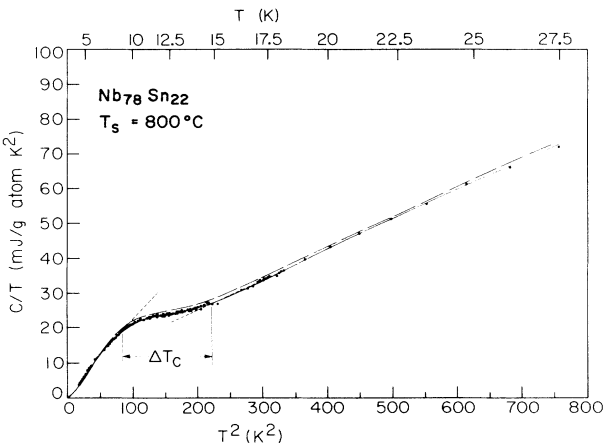


FIG. 2. Specific heat for two 22–at. % Sn Nb-Sn samples. The samples were grown two years apart. The dashed line is taken from the data shown in Fig. 1 for the 22–at. % Sn sample. The deposition rate was 12 Å/sec and the background pressure was $1\times10^{-7}$ Torr. The solid line and data points are for a sample grown at 20 Å/sec and $3\times10^{-7}$ Torr. The construction for determining the transition width is indicated for the solid line.

in order to test the approximation to the transition width described above. The fit was made by using the total lattice specific heat and average electronic specific heat $\gamma$ as determined from the data above $T_c$, and a weighted sum of BCS terms with reasonable values for $\gamma$ and $T_c$ assumed. The 10%-90% points of the weighting gave a width in $T_c$ of 6 K for each; the onset and finish of the transitions were the same as those determined by the previous method to the accuracy that the discreteness of the terms in the sum could allow.

The broad transitions of these Nb-Sn samples are reflected in other bulk measures of the superconductivity, specifically critical currents,[14,18] superconductive tunneling,[15] and rf surface losses.[23] The inductively or resistively measured $T_c$ does not appear broad because these measurements are sensitive to continuous filaments of high-$T_c$ material and are insensitive to regions of low-$T_c$ material between. Even the samples with the broadest transition widths as measured by specific heat show only a 0.7-K width when measured inductively.

A broad transition temperature is an indication of an inhomogeneity in the material properties of the sample. This inhomogeneity must occur on a length scale greater than the Ginzburg-Landau superconducting coherence length $\xi_{GL}$ at $T=0$, which in the A15 superconductors is approximately 50 Å. The factors affecting $T_c$ in these materials are strain, order, composition, and impurities. For reasons to be discussed below, it is believed that an inhomogeneity in composition is the source of the broad $T_c$. If it is assumed that $T_c$ changes nearly linearly with composition, as experiments suggest, then a spread of 5–6 K in transition temperature for Nb-Sn corresponds to a spread in composition of 2–3 at. % Sn.

Figures 3 and 4 show the results for V-Ga and V-Si prepared at 750 and 800 °C, respectively, at 20 Å/sec. The V-Ga system is of particular interest since the A15 structure is the equilibrium phase from 20–30 at. % Ga; hence, the behavior of B-element-poor A15 material may be compared with that of B-element-rich A15 material. Figure 5 summarizes the composition dependence of the

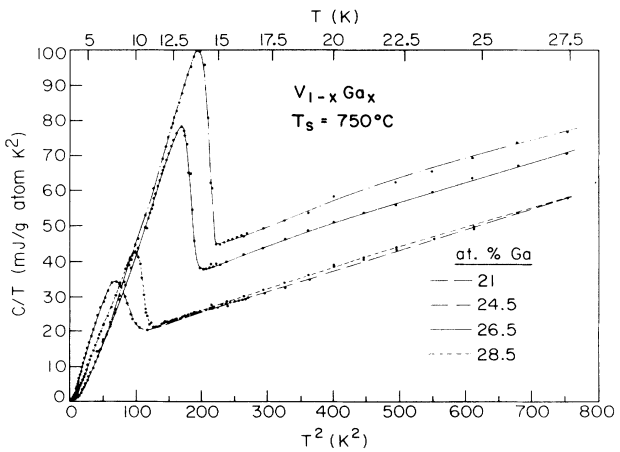


FIG. 3. Specific heat for four samples of A15 V-Ga spanning the phase field. The deposition conditions were $T_s=750$ °C, deposition rate of 20 Å/sec, $P=3\times10^{-8}$ Torr.

transition width for the various $A15$ films measured. Nb-Sn exhibits the largest effect, although it should be noted that the change in $T_c$ with a given change in composition is nearly 50% greater in the Nb-based compounds than in the V-based ones. Hence the maximum width for V-Ga, 2.5 K, implies a composition spread of 1.5–2 at. % Ga, which is two-thirds of the maximum composition spread estimated for Nb-Sn. In the V-Ga system the composition dependence of the transition width is asymmetric about the stoichiometric composition, even though the composition dependence of the transition temperature itself is symmetric. Measurements of the superconductor–insulator–normal-metal (SIN) tunneling spectrum for $A15$ V-Ga of various compositions further support the conclusion; they find an asymmetry in the composition dependence of the breadth of the superconducting gap despite the symmetry in the gap itself.[17] Thus, the origin of the inhomogeneity is itself a function of composition. This seemingly minor statement is sufficient to rule out many proposed explanations of the inhomogeneity.

In order to uncover the origin of the inhomogeneity, its systematics were probed by varying the deposition conditions. The Nb-Sn system was chosen since the effect is greatest here. Figure 6 shows the specific-heat results for the Nb-Sn samples measured before and after an 800-°C anneal for 24 h. Since diffusion in the bulk of the $A15$ materials is expected to proceed by vacancy motion only,[29] annealing at temperatures below half the melting temperature is expected to allow only local motion of the atoms, such as ordering, rather than substantial diffusion. Higher-temperature anneals destroy the doped silicon-on-sapphire devices used to measure the specific heat, and cause excessive Sn loss from thin-film samples, presumably from the grain boundaries and surface of the films. The small changes seen in Fig. 6 are, in fact, a result of an increase in order. The residual resistivity of both samples decreased slightly. This decrease caused no change in the $T_c$ of the stoichiometric sample. It caused a slight increase in $T_c$ of the off-stoichiometric sample, but no decrease in transition width. It is interesting to note the changes in the normal-state specific heat of the off-stoichiometric sample. The increase in $T_c$ is accompanied by a reduction in the slope of $C_p/T$ versus $T^2$, and an increase in the extrapolated intercept of $C_p/T$ to $T=0$. The former corresponds to an increase in the average phonon frequencies, such as the Debye temperature $\Theta_D$. The latter corresponds to an increase in the renormalized electron density of states.

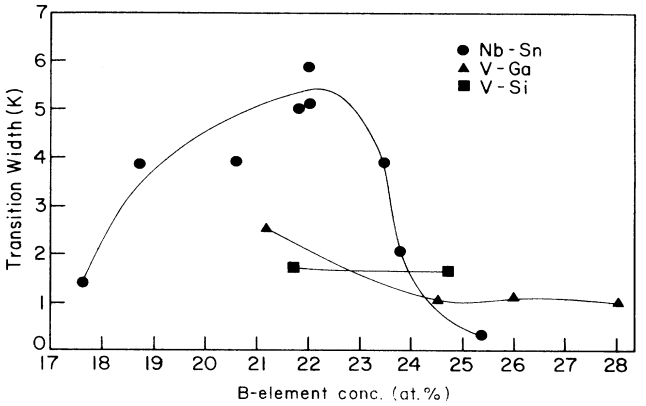


FIG. 5. Composition dependence of the width of the transition temperature as measured by specific heat for Nb-Sn, V-Ga, and V-Si.

To probe the effect of deposition rate on the transition width, a series of three samples were made under nearly identical conditions with deposition rates from 7 to 20 Å/sec. No apparent change in transition width was observed. However, a strong dependence on deposition temperature is found. Nb-Sn samples were grown at temperatures ranging from 200 to 1000 °C, resulting in drastic variations in the surface mobility of the atoms during growth. Samples deposited below 800 °C are less well ordered than those deposited at 800 °C and have corre-

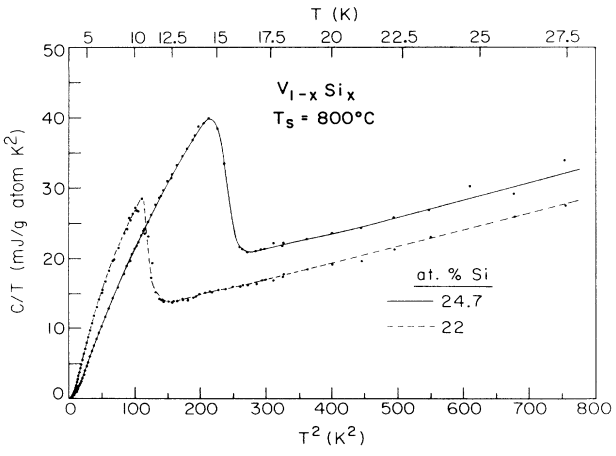


FIG. 4. Specific heat for two samples of $A15$ V-Si spanning the phase field. The deposition conditions were $T_s=800$ °C, deposition rate of 20 Å/sec, $P=3\times10^{-8}$ Torr.

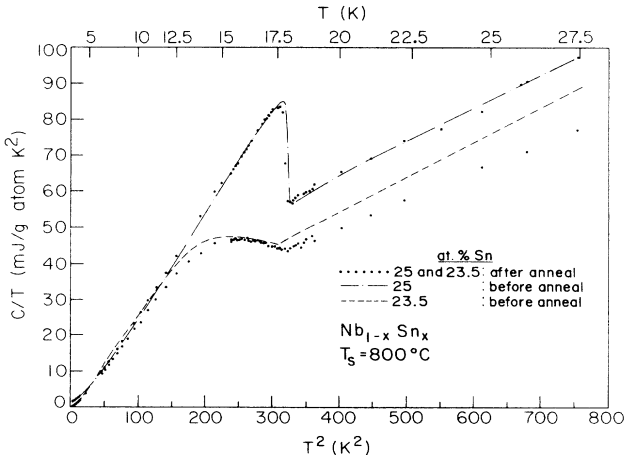


FIG. 6. Specific heat for 25- and 24-at. % Sn Nb-Sn samples grown at 800 °C before and after an anneal at 800 °C for 24 h. Points show data taken after the anneal; lines show data taken before.

spondingly depressed transition temperatures. Therefore, all samples grown at deposition temperatures below 800 °C were subjected to a subsequent *in situ* ordering anneal at 800 °C for 24 h. This anneal brought the inductively measured transition temperature up to that of samples of similar composition grown at 800 °C. As shown in Fig. 6, this anneal has a minimal effect on samples deposited at 800 °C. Samples were not grown at deposition temperatures above 1000 °C due to extreme Sn loss during the evaporation. Figure 7 shows the specific-heat data for two of the off-stoichiometric samples grown below 300 °C and annealed at 800 °C for 24 h. The transition width is reduced to 1.5 K, which we believe may be the intrinsic limit of the homogeneity of the deposition. Figure 8 shows the data for an off-stoichiometric sample grown at 1000 °C. The transition width is approximately 2 K. The solid lines in both Figs. 7 and 8 are taken directly from the lines shown in Fig. 1 for "standard" samples deposited at 800 °C. Results for samples grown at 450 and 600 °C may be found in Ref. 18.

Figure 9 summarizes the transition width versus deposition temperature for three representative compositions, 19–20 at. % Sn, 22 at. % Sn, and 25 at. % Sn. The data for the off-stoichiometric samples exhibit a broad maximum between 600 and 800 °C. The increase in transition width seen in the stoichiometric samples grown at reduced substrate temperatures and subsequently annealed is not understood. The anneal brings the entire inductively measured $T_c^L$ and the onset of the transition measured by specific heat to the full value, but the transition width measured by specific heat is 1.4 K. Our best hypothesis is that some regions of the samples are incompletely ordered even after the 24-h 800-°C anneal. Results on splat-quenched and annealed $Nb_3Pt$ do suggest that ordering may be incomplete after 24 h.[30]

Upon examining the microstructure of the samples grown at 900 °C and above by transmission electron microscopy (TEM), it was discovered that they are single crystal. It was also discovered that certain of the samples grown at 800 °C were single crystal as well, presumably as a consequence of better substrate cleaning or polishing. The vast majority of the 800-°C samples, and all the samples whose specific heat is shown in Figs. 1 and 2, are polycrystalline with an average grain size of several thousand angstroms. References 18 and 20 contain the TEM micrographs and selected-area-diffraction (SAD) images of the single-crystal and polycrystalline samples, as well as a discussion of the characteristic defects in each. Figure 10 compares the specific-heat data for a single-crystal sample grown at 800 °C with a polycrystalline sample of identical composition grown under virtually

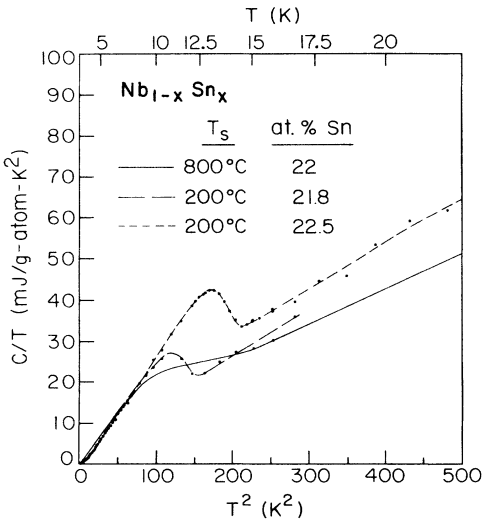


FIG. 7. Specific heat for two Nb-Sn samples grown at a substrate temperature below 300 °C and annealed for 24 h at 800 °C. The solid line shows a standard result for a deposition temperature of 800 °C.

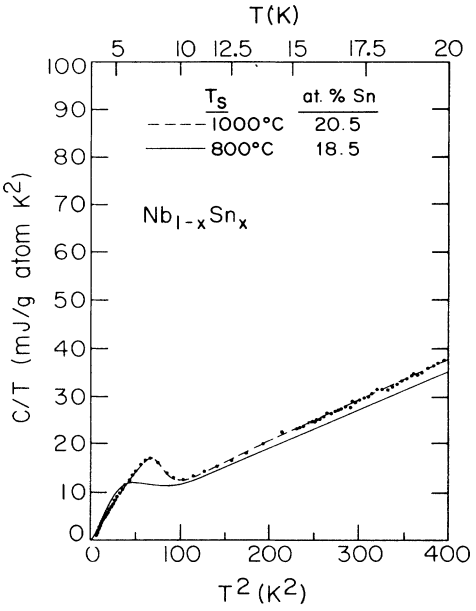


FIG. 8. Specific heat for a Nb-Sn sample grown at 1000 °C. The solid line shows a standard result for a deposition temperature of 800 °C.

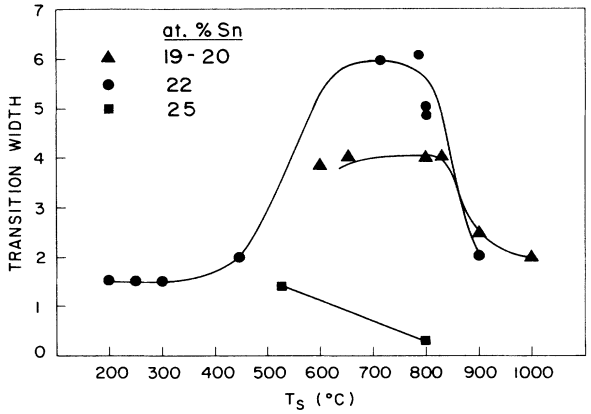


FIG. 9. Deposition temperature dependence of the transition width as measured by specific heat for three compositions of Nb-Sn.

identical deposition conditions. The specific-heat data both above and below $T_c$ are identical, but the transition width of the polycrystalline sample is 4 K, while that of the single-crystal sample is 2 K, very close to the presumed limit of deposition homogeneity. Two other Nb-Sn samples grown at 675 and 750 °C, respectively, during the same period of time also show a slightly reduced transition width. X-ray-diffraction and TEM measurements on these two samples show that, while they are not single crystal, they are more oriented than usual.

A correlation of transition width with microstructure was also seen in superconductive tunneling results on $A15$ V-Ga.[17] Briefly summarizing, a double-gap structure is seen in the tunneling data for Ga-poor samples grown on sapphire substrates. When Ga-poor samples are grown on an amorphous $Si_3N_4$ substrate, the double gap goes away. X-ray measurements show that the former are double-textured (200) and (210), while the latter have no strong texture.

## DISCUSSION

We will first summarize the results presented in the preceding section. Next, we will draw some basic conclusions as to the possible source of the inhomogeneity and will rule out several trivial explanations. We will then present the outline of the model developed to explain the results; the full details will be presented elsewhere. Finally, we will consider a couple of alternate and, we believe, less satisfactory models.

To summarize the results section:

(1) Certain of the $A15$ compounds prepared by electron-beam codeposition onto heated substrates at compositions believed to be metallurgically stable exhibit broad transitions to the superconducting state as measured by specific heat. This broad transition must be due to an inhomogeneity in the material properties of the sample. The inhomogeneity is greatest in off-stoichiometric Nb-Sn, followed by Ga-poor V-Ga. Stoichiometric Nb-Sn has an extremely sharp transition. Ga-rich V-Ga and both stoichiometric and Si-poor V-Si are relatively sharp.

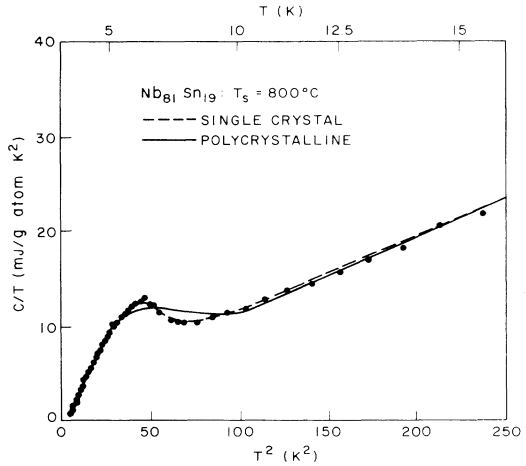


FIG. 10. Specific heat for single-crystal Nb-Sn sample grown at 800 °C. The solid line shows a standard polycrystalline sample also grown at 800 °C.

Figure 5 summarizes these results. Annealing a stoichiometric and a Sn-poor Nb-Sn sample for 24 h at 800 °C leaves both transition widths unchanged, as shown in Fig. 6.

(2) The transition width for off-stoichiometric Nb-Sn does not appear to depend strongly on deposition temperature between $T_s = 600$ and 800 °C or rate between 2.5 and 60 Å/sec. For deposition temperatures of 450 °C and below with subsequent annealing, however, the transition width drops sharply. In addition, for deposition temperatures of 900 °C and above, the width drops sharply. Figure 9 summarizes the dependence of the width on deposition temperature for $A15$ Nb-Sn. The samples grown at 900 °C and above were found to be single crystal.

(3) The transition width correlates with the microstructure. In particular, a single-crystal sample has a transition width much reduced compared to a polycrystalline sample grown under essentially identical conditions, as shown in Fig. 10. Tunneling studies on V-Ga, the results on samples grown at 900 and 1000 °C, and other results discussed in the Results section also support this conclusion.

Nb-Sn samples with the largest transition widths were probed for macroscopic inhomogeneity as follows. A sample was broken into small pieces and the inductive $T_c$ for each piece was measured. Lateral variations in $T_c$ on a large length scale (0.1 in.) would cause these pieces to have different transition temperatures, which they did not. To test for variations in $T_c$ through the sample thickness, the top $\sim 1000$ Å of one sample was chemically etched away and its inductive $T_c$ measured. This etching and measuring sequence was repeated until the sample was completely etched through. Using a technique developed by Howard, a second sample which was deposited on a copper-niobium bilayer was lifted off by etching the copper away.[31] The sample was attached face-down to a substrate and the above etching and measuring procedure was repeated from the back side. No change in the inductive $T_c$ was observed until the samples were less than $\approx 1000$ Å thick. This etching and measuring technique only rules out monotonic variations in $T_c$; it cannot test for fluctuations through the film thickness since the inductive $T_c$ measures the highest-$T_c$ material.

The most likely source of the broad transitions is a local variation in composition. Relatively small variations, on the order of 3 at. % Sn, can change the $T_c$ of $A15$ Nb-Sn by the 6 K found between the onset and finish of the broadest transition. The $T_c$ of $A15$ superconductors can also be influenced by such properties as strain, site-antisite disorder, or impurities. However, producing a 6-K change in the $T_c$ of compositionally homogeneous Nb-Sn by introducing any of these factors requires unreasonably large values. Moreover, it is difficult to image that if strain, disorder, or impurities were large enough to reduce the $T_c$ by 6 K off-stoichiometry, the stoichiometric material would remain untouched. Finally, as will be shown in the next two paragraphs, the temperature and microstructure dependence of the width would be difficult to explain.

Consider first the evidence against strain as the source of the transition width. It is unlikely that a single-crystal

sample would be under significantly less strain than a polycrystalline one, yet Fig. 10 showed that the transition width of the single-crystal sample is less than that of the polycrystalline sample grown under the same conditions. Also, since the primary source of strain is presumably the substrate, the breadth of the transition would be due to a monotonic increase in $T_c$ through the sample, a possibility which was ruled out above.

Consider next the evidence against disorder and impurities. It is difficult to envision any scenario in which samples grown at 800 °C could be substantially less homogeneously ordered or contain more impurities than samples grown both at higher and lower $T_s$. It would, for example, be necessary to postulate that an initially disordered sample, deposited at $T_s \leq 450$ °C, which was then annealed would be more homogeneously ordered than an initially well-ordered sample, deposited at 800 °C, which was also annealed. Finally, since samples grown at different deposition rates, different background pressures, or different ratios of deposition rate to pressure possess identical transition widths, impurities are an unlikely cause. Also, upper limits of tenths of atomic percent impurities (well below the level necessary for a 6-K change in $T_c$) have been set on these films by Auger depth profiling and electron microprobe.

Composition, therefore, is by far the most likely source of the transition width. Careful measurements in an x-ray diffractometer show a broadening of the high-angle peaks in off-stoichiometric Nb-Sn.[16] The peak width and the composition dependence of the width are completely consistent with composition as the origin of the broad transition and with the composition dependence seen in Fig. 5. Electron microprobe, which has a relative accuracy of tenths of an atomic percent, was used to probe for compositional variations on all length scales greater than the minimum probe size of 1 $\mu$m. Samples were tested extensively for lateral compositional inhomogeneity. To probe variations with depth, a sample was ground at a 2° angle to expose successive depths through the sample; again, the electron microprobe was used. In both cases, results were negative. To probe on a still smaller length scale for the inhomogeneity, the samples were examined by scanning transmission-electron microscopy with energy dispersive x-ray analysis (STEM-EDX). The probe size of this method is on the order of 100 Å. Unfortunately, the compositional resolution is only $\pm$ several at. %, which is worse than the expected variation. No inhomogeneity beyond the scatter in the data was found.[16,32]

The most obvious source of a compositional inhomogeneity is an inhomogeneity, either spatial or temporal, in the relative deposition rates of the two elements. Since the transition width is greatly reduced (to 1.5 K) by depositing the samples at low temperatures where the surface diffusion is low, we conclude that the deposition itself is homogeneous enough, both spatially and temporally, to allow a 1.5-K transition width. A caveat must be inserted here. Samples grown at reduced substrate temperatures contain voids and vacancies. Therefore, although no change in transition width was found when samples grown at 800 °C were annealed, it is possible that bulk diffusion is greatly enhanced in samples grown at low temperatures. The reduced transition width *could* therefore be misleading; an inhomogeneity in the deposition of the low-temperature samples could be reduced by the subsequent anneal. In the highest-deposition-temperature samples where, again, the transition width is reduced, an inhomogeneity in the deposition could be removed by the greatly enhanced surface diffusion during growth. There are several arguments against this explanation, however. First, the dependence of the width on microstructure seen in both Nb-Sn and in V-Ga as well as the asymmetry in the V-Ga results is inconsistent with this hypothesis. Second, some of the metastable A15 materials may be grown by depositing the desired composition onto cold substrates and then annealing.[33] This success depends on low bulk diffusion rates. Finally, since the inhomogeneity must exist on a length scale greater than 50 Å, at a deposition rate of 10–20 Å/sec, the rate monitors would easily show a fluctuation of the magnitude necessary to produce a vertical compositional variation. A hypothesized horizontal variation due to shadowing is inconsistent with the large surface mobility found at 800 °C (to be discussed below) and the lack of variation found by microprobe.

Since there is strong evidence that the atoms arrive at the surface relatively homogeneously, the inhomogeneity must occur after the atoms hit the surface. It is very unlikely that it occurs after the film is grown, primarily because bulk diffusion is so slow. We believe that the inhomogeneity occurs at the surface during the growth and is then effectively frozen into the bulk. A variation in the relative sticking coefficient of the two elements due to spatial or temporal variations in the substrate temperature is ruled out on three counts. First, the relative sticking coefficients, at least for Nb and Sn, are independent of substrate temperature up to 900 °C. This statement is based on a series of samples grown only a few minutes apart at different substrate temperatures but identical deposition rates. The resulting compositions, measured by electron microprobe, were identical for samples containing 25 at. % Sn or less grown at substrate temperatures of 900 °C or less. Second, temperature variations laterally along the substrate are unlikely to occur on a length scale smaller than that probed by the electron microprobe and unlikely to remain constant between 600 and 800 °C, yet decrease for samples grown at 900 and 1000 °C. Finally, it has been observed that V-Ga samples annealed for 24–48 h at 800–950 °C show *far* more Ga loss than the observed Sn loss from similarly prepared and annealed Nb-Sn samples, proving that Ga is far more volatile from V-Ga than Sn is from Nb-Sn. This fact implies that any inhomogeneity induced by a variation in sticking coefficient would be greater in V-Ga than Nb-Sn, a conclusion not born out by the evidence, as seen in Fig. 5.

Temperature gradients can also cause composition gradients by a mechanism known as the Soret effect.[34] However, the necessary temperature gradient could not occur on a length scale smaller than 1 $\mu$m, and would be unlikely to have the necessary dependence on substrate temperature. The possibility that the sticking coefficient might depend on surface orientation will be considered below.

The final possibility to be considered before turning to

what appears to be the correct explanation is that the accepted equilibrium phase diagram might be wrong and off-stoichiometric $A15$ Nb-Sn might not be the stable phase. In particular, instead of an equilibrium phase field extending from 18–25 at. %Sn, there could be a spinodal region due to especially stable compositions at 25 at. % Sn and, for example, 18.75 at. % Sn, where one out of every four Sn atoms is replaced by a Nb atom.[35] The inhomogeneity would be due to an incomplete segregation. At low temperatures, this process would be further limited. To explain the high-temperature data, one would have to presume that the entropy term in the free energy caused the spinodal region to end between 800 and 900 °C. This hypothesis, in addition to not explaining the microstructure dependence of the transition width or the lack of change between 800 and 600 °C, is nearly impossible to verify since bulk diffusion rates at 800 °C or below are far too low to permit observation of any segregation in bulk material. In addition, the phase diagram of V-Ga would have to be similar at temperatures near 800 °C, despite the fact that the accepted phase diagram for V-Ga is quite different from that for Nb-Sn. Note that the results *cannot* be explained by simply hypothesizing that the equilibrium phase field is narrower than commonly believed, extending only to 24 at. % Sn on the Sn-poor side of stoichiometry, as the experiments of Schiffman and Bailey on Nb-Sn suggest.[36] In their proposed phase diagram, off-stoichiometric $A15$ Nb-Sn would, in fact, be metastable at the deposition temperatures used, including, incidentally, 900 and 1000 °C. However, the stable configuration would be bcc Nb plus 24 at. % Sn $A15$; segregation in this two-phase field, consisting of two different crystal structures, would be by a precipitation mechanism. Unless the $A15$ phase itself contains a spinodal region, it is energetically impossible to segregate into $A15$ regions containing different Sn concentrations.

We believe that the inhomogeneity is due to a true surface effect. All of the results may be explained by hypothesizing a transfer of Sn between grains growing with different crystallographic orientations. We speak of transferring Sn rather than Nb because it is likely that the surface mobility of Sn is far greater than that of Nb.[16,29,37] We believe that the cause of this transfer is a difference in the relative bonding energies of Sn and Nb at the different orientation surfaces. A difference in bonding energy is known to lead to orientation-dependent surface segregation, a phenomenon frequently seen in alloys of materials such as Nb and Sn with vastly different melting temperatures. A pseudoequilibrium model related to surface segregation but applicable to a growing film will be developed in the next section. A surface-to-surface transfer of one element results in a grain-to-grain variation in composition due to the dynamics of the film growth. The composition dependence of the transition width and the results for the different $A15$ compounds will be discussed after the model is outlined in the next section. We will consider here only how this hypothetical transfer explains the temperature and microstructure dependence.

First, the high-temperature and single-crystal results are immediately explained since only one orientation is present. Consider next the low-deposition-temperature results. The primary effect expected by reducing the substrate temperature is to reduce the surface mobility. This reduction will cause the grain size to be smaller[14,19] and the orientation of the grains to become more random, as well as reducing the distance an atom at the surface can travel before being buried by the incoming flux. The dominant effect on the transition width is believed to be the reduction in grain size. Estimates for surface diffusion constants, to be discussed below, show that root-mean-square diffusion lengths are far greater than the average grain size at all deposition temperatures and rates used. Thus there is sufficient mobility to permit the Sn transfer, and so the inhomogeneity could still exist. However, the grain size is reduced, and so the length scale on which the compositional variation occurs will also be reduced. During the subsequent 24-h anneal, substantial grain growth occurs, leaving the final average grain size near 1000 Å as measured by TEM. The grain growth, which does not require bulk diffusion, should leave the inhomogeneity unaffected. What had been a grain-to-grain variation in composition becomes regions of different composition within a single much larger grain. As long as there is not boundary scattering at the edges of those regions, the proximity effect will reduce the width of the superconducting transition temperature when these regions become comparable to or smaller than the Ginzburg-Landau coherence length at $T=0$. The resistivity of these cold-deposited, annealed films is quite comparable to that of films deposited at high temperature, implying that the mean free path and $\xi(0)$ are also comparable and that there is not much boundary scattering.

This argument implies that when the as-grown grain size is less than $\xi(0)$, the transition width will be reduced even if the magnitude of the inhomogeneity is unaltered. The as-grown average grain size is roughly exponential with deposition temperature. From measurements in Refs. 14, 16, and 19, it is estimated that the crossover from grain diameters being far larger than $\xi(0)$ to far smaller occurs between 600 and 450 °C, the same temperature range where the drop in transition width occurs. In addition, the reduced fraction of grains of low-index orientation at low substrate temperature is likely to reduce the inhomogeneity, for reasons to be discussed below. Finally, any bulk diffusion that does occur during the anneal will be more effective at reducing the inhomogeneity if the length scale of the inhomogeneity is only 30 Å compared to 2000 Å, due to the different as-grown grain sizes.

## MODEL

We will present here only the outline of the model; the details are being presented elsewhere. In materials such as Nb-Sn where one element is far more weakly bonded than the other, surface segregation is likely. In a solid solution of elements $A$ and $B$ randomly distributed on equivalent sites each with $n$ nearest neighbors, the free energy

$$F=E-TS=\tfrac{1}{2}[Nnx^2\varepsilon_{AA}+2Nnx(1-x)\varepsilon_{AB}+Nn(1-x)^2\varepsilon_{BB}]-TS\ , \quad (1)$$

where $x$ is the concentration of element $A$, $N$ is the total number of atoms, and $\varepsilon_{AA}$, $\varepsilon_{AB}$, and $\varepsilon_{BB}$ are the $A-A$, $A-B$, and $B-B$ atomic-bond energies given the nearest-neighbor distance in the alloy. Only nearest-neighbor interactions are included. Including only the entropy of mixing,

$$S=-Nk_B[x\ln x+(1-x)\ln(1-x)]\ . \tag{2}$$

Assuming no reconstruction or relaxation at the surface, these expressions apply both to the bulk material with concentration $x_b$ and to the surface with $x_s$, each with an appropriate number of nearest neighbors $n_b$ and $n_s$. At equilibrium, there can be no gain in free energy by exchanging material between the two; hence,

$$\frac{d(F_s+F_b)}{dx_s}=\frac{d(F_s+F_b)}{dx_b}=0\ .$$

For small changes in concentration,

$$dx_b\approx -dx_s\ .$$

In equilibrium, then,

$$\frac{dF_s}{dx_s}\approx\frac{dF_b}{dx_b}\ . \tag{3}$$

The derivative of Eq. (1) is

$$\frac{dF}{dx}=Nnx(\varepsilon_{AA}+\varepsilon_{BB}-2\varepsilon_{AB})+Nn(\varepsilon_{AB}-\varepsilon_{BB})+Nk_BT\ln\left[\frac{x}{1-x}\right]\ . \tag{4}$$

If the alloy is dilute so both $x_s$ and $x_b\ll 1$, the expression resulting from Eqs. (1)–(4) is the familiar surface segregation result

$$\frac{x_s}{1-x_s}=\frac{x_b}{1-x_b}\exp\left[\frac{(n_b-n_s)(\varepsilon_{AB}-\varepsilon_{BB})}{k_BT}\right]\ . \tag{5}$$

If the alloy is not dilute, then the expression is more complicated:

$$\frac{x_s}{1-x_s}e^{-2x_sn_s\varepsilon/k_BT}=\frac{x_b}{1-x_b}e^{-2x_bn_b\varepsilon/k_BT}\times\exp\left[\frac{(n_b-n_s)(\varepsilon_{AB}-\varepsilon_{BB})}{k_BT}\right]\ , \tag{6}$$

where $\varepsilon$ is the energy of mixing,

$$\varepsilon\equiv\varepsilon_{AB}-\tfrac{1}{2}(\varepsilon_{AA}+\varepsilon_{BB})\ .$$

Equation (5) says that the concentration of the more weakly bonded element will be enhanced at the surface in comparison to the bulk. This model neglects many effects; in particular, it neglects any alteration of bond energy at the surface due to relaxation of the atomic positions. It is, however, sufficient to justify that surface segregation can, in principle, occur when the strengths of the bonds for $A$ and $B$ are different. For a full discussion of surface segregation and reviews of experimental results, see, for example, Kelley and Ponec,[38] Miedema,[39] Chelikowsky,[40] or Overbury *et al.*[41]

When two surfaces of different orientation are in equilibrium, it is quite simple to derive a similar expression relating the concentration on surface 1 with that on surface 2 for a dilute alloy:

$$\frac{x_{s_1}}{1-x_{s_1}}=\frac{x_{s_2}}{1-x_{s_2}}\exp\left[\frac{(n_{s_2}-n_{s_1})(\varepsilon_{AB}-\varepsilon_{BB})}{k_BT}\right]\ . \tag{7}$$

When two neighboring grains are in equilibrium with each other, Eqs. (5) and (7) are satisfied when the bulk of each contains the same concentration ($x_{b_1}=x_{b_2}$) and each of the surfaces have a concentration described by Eq. (5).

If the two grains start at the same concentration and $n_{s_1}\neq n_{s_2}$, a transfer of one element must occur to allow $x_{b_1}=x_{b_2}$ and $x_{s_1}\neq x_{s_2}$. The amount of material transferred is proportionate to the number of surface atoms divided by the number of bulk atoms and hence is negligible unless the volume of each grain is extremely low. If, for example, the "grains" were only one unit cell thick, Eq. (7) would be satisfied by transferring one element from one "grain" to the other. Upon adding a second unit cell of material to each grain, the top layer would deplete the underlying layer, resulting in both Eqs. (5) and (7) being satisfied and $x_{b_1}=x_{b_2}$.

If the added layer is unable to deplete the underlying layer, then the surface transfer between "grains" which occurred in the first layer would simply recur. As layers continue to be added, the grains would grow with unequal bulk compositions, but would continue to satisfy Eq. (7). This process requires that the two surfaces be in equilibrium with each other; hence, Eq. (7) applies, but the surface of each grain must be out of equilibrium with the bulk, and, hence, Eq. (5) is not satisfied.

Given the different bonds at the surface and in the bulk, the requirements of low bulk mobility and high surface mobility may be easily met under standard deposition conditions. For example, measurements of isotope bulk diffusion constants $D_b$ in the transition metals Ni, Fe, and Co indicate that at a reduced temperature of $T/T_M=0.4$, where $T_M$ is the melting temperature (for $Nb_3Sn$, this implies $T=800\,^\circ$C), $D_b\simeq 8\times10^{-20}$ cm$^2$/sec.[42] Measurements have been made on bulk diffusion in $V_3Ga$.[43] Van Winkel *et al.* found that Ga essentially did not diffuse at all at temperatures near 800 °C, a result consistent with calculations by Welch *et al.* on the diffusion of Sn through $Nb_3Sn$.[29] The diffusion constant of V at 800 °C is $\approx 1\times10^{-20}$ cm$^2$/sec, which is even less than that predicted by the transition-metal isotope diffusion. Extremely limited data exist on surface diffusion constants at high temperature. By extrapolating isotope diffusion constants for transition metals measured at room temperature, we estimate $D_s\approx 1\times10^{-6}$ to $1\times10^{-7}$ cm$^2$/sec.[44] The estimate for surface diffusion lengths is supported in the $A15$ materials by measurements made on the separation of second-phase inclusions in Nb-Sn grown with a composition lying in the two-phase $A15$-plus-$\sigma$ region.[16] It is also entirely consistent with measurements of Pd distribution as a function of time on a W surface at 800 °C.[45] At typi-

cal deposition rates, a surface layer is buried in 1 sec. In 1 sec, assuming a random walk diffusion process, an atom in the bulk has a root-mean-square diffusion length of less than a tenth of an angstrom, while on the surface, the length is many micrometers. These distances easily justify the idea of surfaces which are thousands of angstroms apart being in equilibrium with each other, while being out of equilibrium with bulk material only angstroms away.

The $A15$ crystal structure is unfortunately more complicated than that of a simple alloy in which all sites are equivalent. At the stoichiometric $A_{0.75}B_{0.25}$ composition, the $A15$ crystal structure consists of a bcc lattice of the $B$ element with nonintersecting chains of the $A$ element along each face. In maximally ordered $B$-element-*poor* $A15$ compounds, the $A$ sites are all filled with $A$-element atoms, while the $B$ sites contain either $A$ or $B$, depending on the sample composition. In maximally ordered $B$-element-*rich* $A15$ compounds, the $B$ sites are filled with $B$-element atoms, while the $A$ sites contain $A$ or $B$. Based on the work by Welch *et al.* on $A15$ Nb-Sn,[29] the only significant contribution to the $B$-site bonding energy is due to the nearest $A$ sites. This coordination will be written as $n^B$ and is equal to 12 in the bulk. For the $A$ site, the nearest-neighbor $A$ sites, the next-nearest-neighbor $A$ sites, and the nearest $B$ sites all contribute relatively equal bonding energies.[29] These coordination numbers will be written as $n^{A1}$, $n^{A2}$, and $n^{A3}$, respectively. In the bulk, $n^{A1}=2$, $n^{A2}=8$, and $n^{A3}=4$. These bonds will be broken to different extents at different surfaces.

It is also necessary to consider that $\varepsilon_{AB}$, $\varepsilon_{BB}$, and $\varepsilon_{AA}$ depend on the atomic separation. There are three relevant distances, the $A$ site to $B$ site, the $A$ site to nearest-neighbor $A$ site, and the $A$ site to next-nearest-neighbor $A$ site, defined to be $r_{AB}$, $r_{A1}$, and $r_{A2}$, respectively. Thus, for example, $\varepsilon_{AB}(r_{AB})$ is the $A$—$B$ bonding energy for the atomic spacing corresponding to the $A$- to $B$-site distance.

We will consider $B$-element-poor and $B$-element-rich material separately. This derivation follows the derivation above for a simple alloy, but the expressions are far more complex. Consider first the $B$-element-poor material. The energy $E$ may be written

$$E=\tfrac{1}{2}Nxn^B\varepsilon_{AB}(r_{AB})+\tfrac{1}{2}N(0.25-x)n^B\varepsilon_{AA}(r_{AB})+\frac{0.75}{2}N\left[\frac{x}{0.25}n^{A3}\varepsilon_{AB}(r_{AB})+\frac{0.25-x}{0.25}n^{A3}\varepsilon_{AA}(r_{AB})\right]+\frac{0.75}{2}N[n^{A1}\varepsilon_{AA}(r_{A1})+n^{A2}\varepsilon_{AA}(r_{A2})]\ ,$$

where $x$ is, by tradition, the concentration of element $B$ and we have assumed a random distribution of the excess (beyond 75 at. %) $A$ atoms on the $B$ sites. The first two terms are associated with the bonding energy to the $A$ atoms on the $A$ sites of the $B$ and $A$ atoms, respectively, on the $B$ site. The second two terms represent the bonding energy of the $A$ atoms on the $A$ sites to the $A$ or $B$ atoms on the $B$ site. These terms are an artifact of the double counting of the bonds and are identically equal to the first two terms since $n^B=3n^{A3}$. Henceforth, they will be added together. The last two terms are due to the bonding energy of the $A$ atoms on the $A$ sites and are independent of composition for $x<0.25$.

The configurational entropy of the $A15$ phase for $x<0.25$ is

$$S=k_B\ln\left[\frac{(N0.25)!}{[N(0.25-x)]!(Nx)!}\right]=Nk_B[0.25\ln 0.25-(0.25-x)\ln(0.25-x)-x\ln x]\ .$$

Taking the derivative with respect to changes in composition, we derive the surface-to-surface equation analogous to Eq. (7):

$$Nn_1^B[\varepsilon_{AB}(r_{AB})-\varepsilon_{AA}(r_{AB})]+Nk_BT\ln\left[\frac{x_{s_1}}{0.25-x_{s_1}}\right]=Nn_2^B[\varepsilon_{AB}(r_{AB})-\varepsilon_{AA}(r_{AB})]+Nk_BT\ln\left[\frac{x_{s_2}}{0.25-x_{s_2}}\right]\ . \tag{8}$$

Rearranging,

$$\frac{x_{s_1}}{0.25-x_{s_1}}=\frac{x_{s_2}}{0.25-x_{s_2}}\exp\left[\frac{(n_2^B-n_1^B)[\varepsilon_{AB}(r_{AB})-\varepsilon_{AA}(r_{AB})]}{k_BT}\right]\ . \tag{9}$$

Note that this expression has the structure of Eq. (7). Equation (7) was an approximation good only in the dilute limit, while Eq. (9) did not require $x\ll 1$, or $0.25-x\ll 1$. This simplification is due to the fact that only the $A$-site to $B$-site bonds are relevant, and the $A$ sites are entirely filled by $A$ atoms.

The energy difference $\varepsilon_{AB}(r_{AB})-\varepsilon_{AA}(r_{AB})$ is just the difference between the $A$—$B$ bond and the $A$—$A$ bond at the equilibrium $A$- to $B$-site separation. Welch *et al.* discuss the strengths of these bonds in the Nb-Sn system

and how these strengths affect the theoretical width of the equilibrium $A15$ phase field.[29] Assuming the phase diagram of Charlesworth *et al.*[46] to be correct,the Nb-Nb potential must be stronger at all separations. Therefore,

$$|\varepsilon_{\text{Nb-Sn}}| < |\varepsilon_{\text{Nb-Nb}}| \ .$$

By the same logic,

$$|\varepsilon_{\text{V-Ga}}| < |\varepsilon_{\text{V-V}}| \quad \text{and} \quad |\varepsilon_{\text{V-Si}}| < |\varepsilon_{\text{V-V}}| \ .$$

At equilibrium, the surface-to-bulk expression equivalent to Eq. (5) predicts that surface segregation will occur in the $A15$ system. In particular, the surfaces should show an enhancement of the $B$ element when the overall composition is $B$-element poor. Surface segregation has been looked for in stoichiometric $Nb_3Sn$ and other $A15$ compounds and apparently has not been seen in the absence of oxygen,[47,48] but has not been looked for in off-stoichiometric material. Evidence of Sn segregation to grain boundaries, which, of course, also break bonds, does exist.[49,50]

Next, we must consider how many of the $B$-site bonds are broken at the various surfaces and which surfaces are present during growth. Polycrystalline Nb-Sn has been observed by transmission-electron microscopy to grow on $(1\bar{1}02)$ sapphire primarily in the (100) orientation, with a substantial fraction of the remaining grains in a (311) orientation.[51] Note that for the $A15$ structure, the (100) is the close-packed surface. V-Ga has been observed to grow primarily (100) and (210) (Ref. 17) and V-Si primarily (210).[52] On the (100) surface, there are eight of the 12 bonds. On the (210) surface, there are seven of the 12, and on the (311) surface, there are six of the 12.

Equation (9) predicts a transfer of Sn from the close-packed (100) grain surfaces of Nb-Sn to the (311) surfaces and a transfer of Ga from the (100) grain surfaces of V-Ga to the (210) surfaces. When Nb-Sn is grown on (0001) sapphire, the preferred orientations change to (100) and (210). There is limited evidence from the width of the high-angle x-ray-diffraction peaks that the inhomogeneity is reduced in this case, a result expected from this model since $n^B_{100}-n^B_{210}<n^B_{100}-n^B_{311}$. When V-Ga is grown on $a$-$Si_3N_4$, x-ray diffraction shows no obvious preferential ordering.[17] The sample must have a high fraction of high-index orientations. The model predicts a much reduced inhomogeneity in this case, a result seen in the reduced gap width from the tunneling spectroscopy.[17] Without knowing the energy differences $|\varepsilon_{AA}|-|\varepsilon_{AB}|$ better, it is difficult to compare the different $A15$ compounds with each other. However, the greatest inhomogeneity is expected for the (100) and (311) combination (Nb-Sn), the next largest for (100) and (210) (V-Ga), and the least for (210) and a high-index orientation (V-Si). This progression is reflected exactly by the transition widths of $B$-element-poor Nb-Sn, V-Ga, and V-Si seen in Fig. 5.

When the surface with the higher-index orientation reaches stoichiometry (or, alternatively, if the starting material is stoichiometric or $B$-element rich, such as Ga-rich V-Ga), the $B$ sites are filled by $B$ atoms. If the transfer process were to continue, either the $B$-element-rich grain must phase-segregate into $A15$ plus $\sigma$ phases or else the extra $B$ atoms must sit on $A$ sites in the $A15$ phase. Nucleation of a second phase seems unlikely to be energetically favorable, and hence we will now consider the energetics of putting $B$ atoms on $A$ sites.

The energy $E$ of the $B$-element-rich material is complicated:

$$\begin{aligned}
E=&\frac{N}{2}0.25n^B\left[\varepsilon_{AB}(r_{AB})\frac{1-x}{0.75}+\varepsilon_{BB}(r_{AB})\frac{x-0.25}{0.75}\right]\\
&+\frac{N}{2}(1-x)\left[n^{A1}\varepsilon_{AA}(r_{A1})\frac{1-x}{0.75}+n^{A2}\varepsilon_{AA}(r_{A2})\frac{1-x}{0.75}+n^{A3}\varepsilon_{AB}(r_{AB})\right]\\
&+\frac{N}{2}(1-x)\left[n^{A1}\varepsilon_{AB}(r_{A1})\frac{x-0.25}{0.75}+n^{A2}\varepsilon_{AB}(r_{A2})\frac{x-0.25}{0.75}\right]\\
&+\frac{N}{2}(x-0.25)\left[n^{A1}\varepsilon_{AB}(r_{A1})\frac{1-x}{0.75}+n^{A2}\varepsilon_{AB}(r_{A2})\frac{1-x}{0.75}+n^{A3}\varepsilon_{BB}(r_{AB})\right]\\
&+\frac{N}{2}(x-0.25)\left[n^{A1}\varepsilon_{BB}(r_{A1})\frac{x-0.25}{0.75}+n^{A2}\varepsilon_{BB}(r_{A2})\frac{x-0.25}{0.75}\right] .
\end{aligned}$$

The first two terms in this expansion are due to the bonds between the $B$ sites, which are entirely occupied by $B$ atoms, and the $A$ sites, which are mixed according to composition. The remaining terms are due to the $A$-site bonds. The first three represent $A$ atoms on $A$ sites interacting with other $A$ atoms on $A$ sites and $B$ atoms on $B$ sites. The next two terms represent $A$ atoms on $A$ sites interacting with the extra $B$ atoms on $A$ sites. The next five terms represent the same bonds as the previous five, but for $B$ atoms on $A$ sites. The double counting of bonds by this method is, as usual, eliminated by the factor of $\frac{1}{2}$ at the front of each term.

Taking the derivative,

$$\frac{dE}{dx} = Nn^{A3}[\varepsilon_{BB}(r_{AB}) - \varepsilon_{AB}(r_{AB})] - \frac{N}{0.75}[n^{A1}\varepsilon_{AA}(r_{A1}) + n^{A2}\varepsilon_{AA}(r_{A2})]$$
$$+ N[n^{A1}\varepsilon_{AB}(r_{A1}) + n^{A2}\varepsilon_{AB}(r_{A2})]\frac{1.25}{0.75} - \frac{N}{3}[n^{A1}\varepsilon_{BB}(r_{A1}) + n^{A2}\varepsilon_{BB}(r_{A2})]$$
$$+ \frac{Nx}{0.75}[n^{A1}\varepsilon_{AA}(r_{A1}) + n^{A2}\varepsilon_{AA}(r_{A2})] - \frac{2Nx}{0.75}[n^{A1}\varepsilon_{AB}(r_{A1}) + n^{A2}\varepsilon_{AB}(r_{A2})]$$
$$+ \frac{Nx}{0.75}[n^{A1}\varepsilon_{BB}(r_{A1}) + n^{A2}\varepsilon_{BB}(r_{A2})] \ .$$

Note that unlike $dE/dx$ for the Sn-poor material, this expression depends on $x$ and thus the surface-segregation process will be described by the more complicated form of Eq. (6). In addition of course, there are now many bonds and energies to be considered.

Let us consider the number of bonds present at the various surfaces. We will concentrate on the (210) and (100) surfaces because these are the surfaces relevant to $A15$ V-Ga, the only $A15$ considered in this work which is thermodynamically stable for $x > 0.25$. A complication is introduced by the fact that, referenced to the surface, there are two types of $A$ sites: those that lie in chains which intersect the surface and those that lie in chains parallel to the surface. Table I shows the number of bonds present for each of the three bonds for each type of $A$ site for the (210) and (100) surfaces. The number of each type of bond in the bulk is also shown. By simply counting the number of broken bonds, neglecting the relative strengths of each bond, the (210) surface breaks *fewer* $A$-site bonds than the (100). This situation is the opposite to that found in Ga-poor $A15$ material due to the different relevant bonds. More knowledge of the bond strengths is needed to actually estimate the segregation process, but it is certainly plausible that above and below stoichiometry the driving force will not be the same. The model thus accounts for the reduction in inhomogeneity seen on-stoichiometry in both Nb-Sn and V-Ga and seen in Ga-rich V-Ga.

The phase boundary at 18 at. % Sn for $A15$ Nb-Sn, where the inhomogeneity was also seen to be reduced, is qualitatively different from that at 25 at. % Sn. The $B$ element sites could accommodate more Nb. The energy of mixing of Nb with $A15$ $Nb_3Sn$ controls the composition of this phase boundary. If the transfer of Sn were to occur at 18 at. % Sn overall, one grain would end up below 18 at. % Sn. It would then presumably be energetically favorable to decompose into the $\alpha$-Nb (bcc) phase plus the 18-at. % Sn $A15$ phase, a process which costs boundary energy and would, of course, affect the surface-segregation process. It is not clear how to consider even classic surface segregation at a phase boundary. In addition, it is possible experimentally to have not seen small amounts of bcc phase, either by x-ray diffraction or by the specific heat, especially since the $T_c$ of the bcc phase, which contains $\approx 3$ at. % Sn at its boundary, is the same as the $T_c$ of the 18-at. % Sn $A15$ phase.

A final comment is that the presence of oxygen or any contaminant present during deposition may be expected to change the bond strengths. In particular, since the Nb—O bond is presumably stronger than the Sn—O, the energy difference at two surfaces between putting a Sn or a Nb atom on a Sn site is likely to be reduced by the presence of oxygen. The specific heats of Nb-Sn samples grown with an $O_2$ partial pressure of $\approx 1 \times 10^{-6}$ Torr do, in fact, show a somewhat reduced transition width.[16]

It should be noted here that there are other possible, though to our minds less convincing, causes of a grain-to-grain variation in composition. There could be surface-orientation-dependent reevaporation of Sn, for example, leading to an orientation-dependent sticking coefficient. However, as the transition width decreases with decreasing temperature, this explanation would imply an increased average sticking coefficient. Since the average composition for a given set of rates is independent of deposition temperature below 900 °C, this explanation is ruled out. In addition, it is not obvious why the sticking coefficient would be more homogeneous in Ga-rich V-Ga than in Ga-poor V-Ga.

The next possibility is that even though all the Sn is eventually incorporated, orientation-dependent surface

TABLE I. Number of bonds for $A$ site in bulk and at each surface.

| | Number of bonds to $B$ site | to nearest $A$ site | to next-nearest $A$ site |
|---|---|---|---|
| In bulk | 4 | 2 | 8 |
| (100) surface | | | |
| Chain ∥ to surface | 3 | 2 | 4 |
| Chain ⊥ to surface | 2 | 1 | 4 |
| (210) surface | | | |
| Chain ∥ to surface | 2 | 2 | 5 |
| Chain at an angle to surface | 3 | 1 | 4 |

diffusion constants cause the incorporation rate to vary spatially due to the presence of differently oriented grains. This argument is an entirely kinetic one; it depends on the two grains and the two surfaces being out of equilibrium with each other. Specifically, it might be expected that if an atom were moving slowly over one grain and more quickly over a grain of a different orientation, it would be more likely to be incorporated into the former. Surface diffusion constants are likely to be greatest over the close-packed (100) surface, and decrease for other orientations. The higher-order orientations would therefore be more likely to incorporate a Sn atom than the close-packed orientations. The argument against this explanation lies in the composition dependence of both Nb-Sn and V-Ga. At an average composition of 18 at. % Sn, the grains with the slowest surface diffusion should still incorporate extra Sn, forcing the composition of the close-packed grain into the two-phase bcc + $A15$ range, a result which is not seen, although, again, small amounts of bcc phase would not be observed. Second, it seems again unlikely that diffusion constants would be more homogeneous in Ga-rich V-Ga than they are in the Ga-poor material.

In addition to the above mechanisms, we have considered numerous other possible origins of an inhomogeneity. In particular, since there is no direct evidence for the grain-to-grain variation, a radial distribution of $T_c$ within each grain, independent of orientation, was considered. There are a variety of possible sources for such a distribution. However, for reasons similar to the arguments already outlined in this paper, we feel that these alternate models do not explain the observed results. One overall comment is that, as mentioned previously, the slow bulk diffusion and lack of change with annealing strongly suggest that the inhomogeneity occurs at the surface during the growth. This comment must be considered when proposing any alternate model based on the presence of grain boundaries.

## CONCLUSION

The specific heat of various metallurgically stable $A15$ superconductors grown by electron-beam coevaporation has been measured. These films, which were grown under conditions that would have been expected to produce relatively homogeneous films, have been found to be inhomogeneous as evidenced by a broad $T_c$. Nb-Sn presents the most extreme case of this inhomogeneity, producing a width in $T_c$ ranging from a low of 0.3 K in the stoichiometric 25–at. % Sn material, to a high of 6 K for 22–at. % Sn material. The inhomogeneity may be greatly reduced by growing the samples at low substrate temperatures or by growing single-crystal samples. A model for a novel manifestation of surface segregation has been developed which explains all results found thus far. This model depends on the high surface mobility and low bulk mobility commonly found at deposition temperatures near half the melting temperature. It must be noted, however, that we have no direct evidence of a grain-to-grain variation in composition. The model presented explains results for which it has not been possible to find an alternate viable explanation. Nonetheless, alternate explanations may exist; more experiments, preferably on a completely different set of compounds, of which there are many candidates, would be helpful in establishing the credibility and generality of the model which has been proposed.

## ACKNOWLEDGMENTS

We would like to thank D. A. Rudman, R. Bormann, M. R. Beasley, S. J. Bending, R. S. Howland, and R. H. Hammond for useful discussions on the topic of $A15$ film growth, Conyers Herring for his input on the surface-segregation process, and A. F. Marshall for the TEM work and discussions of the microstructure. This work was supported by the U.S. Air Force Office of Scientific Research under Contract No. F49620-83-C-0014.

---

*Present address: AT&T Bell Laboratories, Murray Hill, N.J. 07974.

†Also at: Bell Communications Research, Inc., Navesink, N.J. 07701.

[1]R. Flükiger, in *Superconductor Materials Science: Metallurgy, Fabrication and Applications*, edited by S. Foner and B. B. Schwartz (Plenum, New York, 1981), p. 511.

[2]L. J. Vieland and A. W. Wicklund, Phys. Rev. **166**, 424 (1967).

[3]A. Junod, J.-L. Staudenmann, J. Muller, and P. Spitzli, J. Low. Temp. Phys. **5**, 25 (1971).

[4]G. S. Knapp, S. D. Bader, and Z. Fisk, Phys. Rev. B **13**, 3783 (1976).

[5]A. Junod, J. Muller, H. Rietschel, and E. Schneider, J. Phys. Chem. Solids **39**, 317 (1978).

[6]G. R. Stewart, B. Cort, and G. W. Webb, Phys. Rev. B **24**, 3841 (1981).

[7]See reviews by G. R. Stewart and A. Junod, in *Superconductivity in d- and f-Band Metals*, edited by W. Buckel and W. Weber (Kernforschungszentrum, Karlsruhe GmbH, Karlsruhe, 1982), and references therein.

[8]A. Junod, T. Jarlborg, and J. Muller, Phys. Rev. B **27**, 1568 (1983).

[9]G. R. Stewart and B. L. Brandt, Phys. Rev. B **29**, 3908 (1984).

[10]R. H. Hammond, J. Vac. Sci. Technol. **15**, 382 (1978).

[11]R. H. Hammond, IEEE Trans. Magn. **MAG-11**, 210 (1975).

[12]D. F. Moore, Ph.D. thesis, Stanford University, 1978.

[13]T. P. Orlando, J. A. Alexander, S. J. Bending, J. Kwo, S. J. Poon, R. H. Hammond, M. R. Beasley, E. J. McNiff, Jr., and S. Foner, IEEE Trans. Magn. **MAG-17**, 368 (1981).

[14]J. Talvacchio, Ph.D. thesis, Stanford University, 1982.

[15]D. A. Rudman, F. Hellman, R. H. Hammond, and M. R. Beasley, J. Appl. Phys. **55**, 3544 (1984).

[16]F. Hellman, Ph.D. thesis, Stanford University, 1985. Note: raw data for all specific-heat plots are available upon request.

[17]S. J. Bending, M. R. Beasley, and C. C. Tsuei, Phys. Rev. B **30**, 6342 (1984).

[18]F. Hellman, A. F. Marshall, J. Talvacchio, and T. H. Geballe, Adv. Cry. Eng.—Mater. **32**, 593 (1986).

[19]B. E. Jacobsen, R. H. Hammond, T. H. Geballe, and J. R. Salem, J. Less-Common Met. **62**, 59 (1978).

[20]A. F. Marshall, F. Hellman, and B. Oh, Mater. Soc. Proc. Ser. **37**, 517 (1985).

[21]D. A. Rudman and M. R. Beasley, Phys. Rev. B **30**, 2590 (1984).
[22]T. P. Orlando, E. J. McNiff, Jr., S. Foner, and M. R. Beasley, Phys. Rev. B **19**, 4545 (1979).
[23]L. H. Allen, W. J. Anklam, M. R. Beasley, R. H. Hammond, and J. P. Turneaure, IEEE Trans. Magn. **MAG-21**, 525 (1985).
[24]S. R. Early, Ph.D thesis, Stanford University, 1981.
[25]S. R. Early, F. Hellman, J. Marshall, and T. H. Geballe, Physica **107B**, 327 (1981).
[26]A. Junod (private communication).
[27]*Superconductivity,* edited by R. D. Parks (Dekker, New York, 1969).
[28]J. M. Daams and J. P. Carbotte, J. Low Temp. Phys. **43**, 263 (1981).
[29]D. O. Welch, G. J. Dienes, O. W. Lazareth, Jr., and R. D. Hatcher, J. Phys. Chem. Solids. **45**, 1225 (1984).
[30]D. Dew-Hughes, J. Phys. Chem. Solids **41**, 851 (1980).
[31]R. E. Howard, Appl. Phys. Lett. **33**, 1034 (1978).
[32]J. Greggi, J. R. Gavaler, and F. Hellman, Bull. Am. Phys. Soc. **30**, 608 (1985).
[33]R. Bormann, D.-Y. Yu, R. H. Hammond, A. F. Marshall, and T. H. Geballe, in *Proceedings of the 5th International Conference on Rapidly Quenched Metals, Wurzburg* (Elsevier, Amsterdam, 1985).
[34]See, for example, A. R. Allnatt and A. V. Chadwick, Chem. Rev. **67**, 681 (1967).
[35]There could even be a series of intermediate compounds, each separated by a spinodal region, corresponding to the ordering of the Nb atoms on the Sn sites. In fact, since at equilibrium the entropy $S$ must equal zero at $T=0$, in theory these intermediate ordered off-stoichiometric $A15$ phases must exist, if the $A15$ is the equilibrium phase at $T=0$.
[36]R. A. Schiffman and D. M. Bailey, High Temp. Sci. **15**, 165 (1982).
[37]K. Togano, T. Asano, and K. Tachikawa, J. Less-Common Met. **68**, 15 (1979).
[38]M. J. Kelley and V. Ponec, Prog. Surf. Sci. **11**, 139 (1981).
[39]A. R. Miedema, Z. Metallkd. **69**, 455 (1978).
[40]J. R. Chelikowsky, Surf. Sci. Lett. **139**, L197 (1984).
[41]S. H. Overbury, P. A. Bertrand, and G. A. Somorjai, Chem. Rev. **75**, 547 (1975).
[42]P. Haasen, *Physical Metallurgy* (Cambridge University Press, Cambridge, 1978) (English translation).
[43]A. Van Winkel, M. P. H. Lemmens, A. W. Weeber, and H. Bakker, J. Less-Common Met. **99**, 257 (1984).
[44]G. Ehrlich, in *Proceedings of the 9th International Vacuum Congress and 5th International Conference on Solid Surfaces,* edited by J. L. de Segovia (ASEVA, Madrid, 1983), p. 3.
[45]H. Wagner, in *Surface Mobilities on Solid Materials,* edited by Vu Thien Binh (Plenum, New York, 1981), p. 161.
[46]J. P. Charlesworth, I. MacPhail, and P. E. Madsen, J. Mater. Sci. **5**, 580 (1970).
[47]H. Ihara, Y. Kimura, H. Okumura, K. Senzaki, and S. Gonda, Adv. Cry. Eng.—Mater. **30**, 589 (1984).
[48]J. Talvacchio, A. I. Braginski, M. A. Janocko, and S. J. Bending, IEEE Trans. Magn. **MAG-21**, 521 (1985).
[49]M. Suenaga and W. Jansen, Appl. Phys. Lett. **43**, 791 (1983).
[50]M. Suenaga, in *Superconductor Materials Science,* edited by S. Foner and B. Schwartz (Plenum, New York, 1981), Chap. 4.
[51]A. F. Marshall (private communication).
[52]D. F. Moore, R. B. Zubeck, J. M. Rowell, and M. R. Beasley, Phys. Rev. B **20**, 2721 (1979).